Inorganic Chemistry

Article

pubs.acs.org/IC

Iron and Manganese Pyridoxal-Based Complexes as Fluorescent Probes for Nitrite and Nitrate Anions in Aqueous Solution

Maria Strianese,[†] Stefano Milione,*[,†] Valerio Bertolasi,[‡] and Claudio Pellecchia[†]

[†]Dipartimento di Chimica, Università di Salerno, via Giovanni Paolo II 132, I-84084 Fisciano, Salerno, Italy

[‡]Centro di Strutturistica Diffrattometrica, Dipartimento di Scienze Chimiche e Farmaceutiche, Università di Ferrara, Via L. Borsari 46, I-44100 Ferrara, Italy

Supporting Information

ABSTRACT: Water-soluble iron and manganese pyridoxal-based complexes $pyr_2enFeCl$ (**1**) and $pyr_2enMnCl$ (**2**) (pyr_2en = *N*,*N*′-ethylenebis(pyridoxylideneiminato) have been synthesized and characterized. Proof-of-principle results that the title complexes can be efficiently used as fluorescent probes for nitrite and nitrate detection are provided. The fluorescent complex $pyr_2enFeCl$ (**1**) selectively recognizes nitrate anions by fluorescent enhancement in an aqueous solution displaying high binding affinities. ESI-MS experiments clearly show the binding of these anions via the substitution of the chloride anion at the metal center. The pyridoxal-based manganese complexes of NO_2^- and NO_3^- have been isolated, and their structures have been established by single-crystal XRD. Density functional theory (DFT) calculations show that the substitution of the chloride anion at the metal center by the nitrite or nitrate anion is favored by the gain in the energies of hydration.

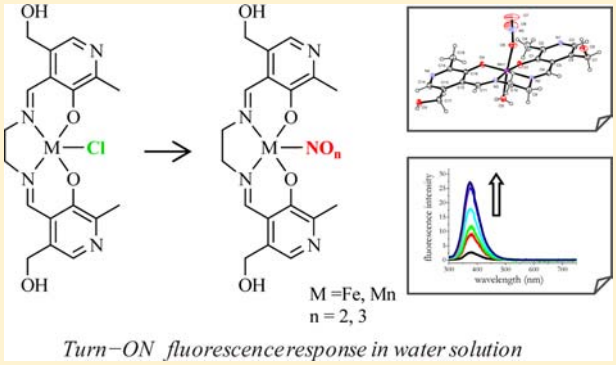

Turn−ON fluorescence response in water solution

INTRODUCTION

Nitrite (NO_2^-) and nitrate (NO_3^-) have been frequently considered with suspicion although the presence of these inorganic anions in bodily fluids has been known from the beginning of the 20th century.[1] Their negative image is due to the health risks related to their overuse. Nitrites can be converted to carcinogenic nitrosoamines in food products and within the human digestive system. Nitrates, although more stable and less toxic than nitrites, can be readily converted to nitrites by microbial reduction in food products.[2,3] However recent studies on therapeutic use[4] of nitrate and nitrite together with emerging data suggesting possible new roles for these anions in physiology[5] have renewed the interest in these inorganic anions. It is now known that nitrate and nitrite are physiologically recycled to form NO and other bioactive nitrogen oxides representing an important alternative source of NO to the classical L-arginine−NO synthase pathway.[6] Selective tracking of these anions in physiological conditions is particularly relevant to elucidate their complex contributions to both healthy and disease states. There is a consequent demand for techniques that can provide direct, fast, and noninvasive nitrite and nitrate detection. A variety of analytical methods for NO_2^- and NO_3^- detection have been already developed. They are based on sophisticated and expensive chemiluminescent equipment, EPR spectroscopy, electrochemistry, amperometry, ion chromatography, or HPLC.[7−14] These methodologies have several advantages, but they also suffer from limitations like requirement of technical expertise and expensive machinery. Therefore, new sensors with improved properties are needed. In particular, the challenge calls for an easy-to-setup and cheap NO_2^- and NO_3^- sensor. The ability to distinguish one analyte over the other is also highly desirable.

While colorimetric and fluorometric detection methods are the dominant analytical approaches in the fields of medical testing and biotechnology,[15−17] because they often allow for a rapid qualitative and quantitative assessment, still few reports deal with the implementation of optical nitrite and nitrate sensing devices.[18,19] Typically, synthetic receptors bind anions by a combination of electrostatic and hydrogen-bonding interactions.[20−22] These are intrinsically weak, and water can compete with the anion in the binding process. Metal−ligand interactions are in general stronger than H-bond interactions, and the resulting receptors have the potential to discriminate anion from water. Schiff base complexes appeared to be a promising class of efficient chemosensors for anion detection because they can exhibit significant fluorescence quantum yields, can have long-lived triplet states, and, above all, can interact with a wide variety of anions through the coordination to the metal center. One of the limitations of the salen-type based complexes used as molecular receptors is their insolubility (or scarce solubility) in aqueous solution. In the framework of our interest for the development of receptors for

Received: April 28, 2013
Published: September 27, 2013

   dx.doi.org/10.1021/ic401055k | *Inorg. Chem.* 2013, 52, 11778−11786

recognition of biologically relevant anions,[23−25] we recently reported on the use of a salen zinc complex for the selective fluorescent detection of adenosine phosphates over various nucleoside polyphosphates (UTP, CTP, TTP, GTP) and inorganic phosphates.[26] In order to develop water-soluble complexes, our salen ligand of choice was a derivative of pyridoxal with ethylenediamine (pyr_2enH_2 = *N*,*N*′-ethylenebis-(pyridoxylideneiminato). The pyridoxal unit renders the ligand and the resulting metal complexes water-soluble. Furthermore pyridoxal and pyridoxamine are forms of vitamin B6, known cofactors required by many enzymes and nontoxic metabolites.

Interactions of NO_2^- and NO_3^- with iron centers have been widely explored to model heme proteins, which are known to have a strong affinity for NO and its related molecules.[27] Manganese complexes display structures and properties that are similar to the analogous iron complexes. For these reasons, we explored the performance of iron or manganese complexes featuring a pyridoxal-based ligand in the molecular recognition of NO_2^- and NO_3^- via optical techniques.

RESULTS AND DISCUSSION

Preparations of the pyr_2enFeCl (**1**) and pyr_2enMnCl (**2**) were carried out in a one-pot two-step reaction as shown in Scheme 1.

Scheme 1

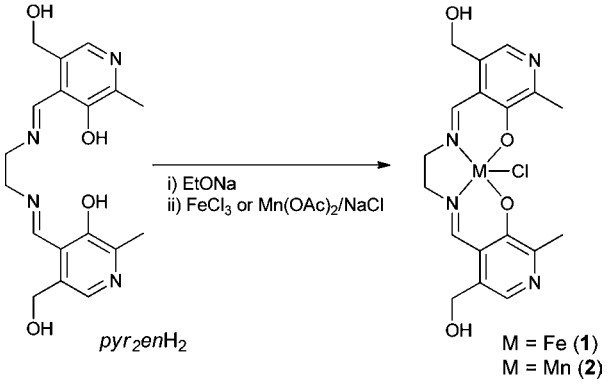

The ferric chloride complex **1** was obtained by treatment of the pyr_2en^{2-} ligand with 1 equiv of $FeCl_3$ in methanol at room temperature. Complex **1** was isolated as a dark brown solid in 52% yield. We succeeded in obtaining single crystals suitable for X-ray diffraction when the crystallization was carried out in a methanol/water solution in the presence of a small amount of chloridric acid. In these conditions, complex **1** was isolated as a HCl adduct (Figure 1). The asymmetric unit consists of two independent HCl adducts, which display very similar geometries, and six molecules of waters, surroundings the adducts and showing some disorder. The complex **1** exhibits a distorted octahedral coordination where the Fe(III) is bonded, in the equatorial plane, to four atoms (N_2O_2) of the pyr_2en ligand. The apical positions are occupied by a Cl^- anion and a water molecule. In both the independent adducts, the bond distances and angles are similar to related octahedral Fe(III) Schiff base complexes[28−31] (Tables S1 and S2, Supporting Information). The crystal packing is dominated by hydrogen bond interactions involving all the water molecules and by a short Cl···Cl interaction of 3.333(6) Å between the coordinated Cl^- anions.

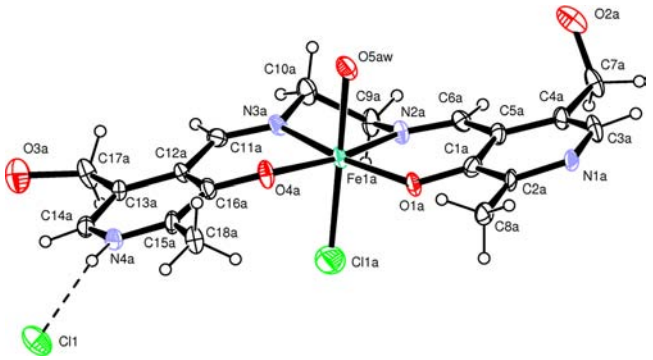

Figure 1. An ORTEP view of the HCl adduct **A** of compound **1** showing the thermal ellipsoids at 30% probability level.

The synthesis of the manganese(III) complex, (pyr_2en)MnCl (**2**), was carried out in good yield by reacting the deprotonated ligand with 1 equiv of $Mn(OAc)_2{\cdot}4H_2O$ and an excess of NaCl in air. The presence of NaCl allows the replacement of acetate anion with the chloride ligand. The successful synthesis of the complex was confirmed by MS (vide infra). Despite several attempts, we could not obtain single crystals of complex **2** suitable for X-ray structure analysis.

Complexes **1** and **2** are thermally stable, and they can be stored indefinitely in the solid state without any precautions to exclude light, air, or moisture.

Solution Structures. Because of the paramagnetism of the metal centers, the ^1H NMR spectra of **1** and **2** showed featureless broad resonances (See Figures S2 and S3 in Supporting Information). We sought evidence for solution structures via electrospray ionization mass spectrometry (ESI-MS). ESI-MS is a soft ionization technique that allows for analysis of solution-phase species in the gas phase without perturbation of their solution distribution. The mass spectrum of **1** showed predominant peaks at 448.15 and 458.19 *m*/*z*. On the bases of simulated mass and isotopic distribution patterns, these peaks were attributed to the species $[(pyr_2en)FeCl + H]^+$ and $[(pyr_2en)Fe + HCO_2H]^+$, respectively. The latter species is probably related to the experimental conditions used to perform the measurement. A less intense peak was observed at 412.2 *m*/*z* corresponding to the species $[(pyr_2en)Fe]^+$. No peak ascribable to dimeric species was detected. The mass spectrum of **2** showed a predominant peak at 410.9 *m*/*z* corresponding to the species $[(pyr_2en)Mn]^+$ and two less intense peaks at 446.9 and 452.0 corresponding to the species $[(pyr_2en)MnCl + H]^+$ and $[(pyr_2en)Mn + CH_3CN]^+$. These data point toward a partial dissociation of chloride anion from the metal center in the polar solvent. Conductivity experiments support this finding. Indeed **1** and **2** were slightly conducting in aqueous solutions: conductivity measurements performed on a 1.00×10^{-3} M solution of **1** or **2** afforded a molar conductivity value of 245 or 153 μS, respectively. Dissociation constants (K_d) were determined by dilution experiments: a K_d value of 3.61×10^{-3} M was found in the case of (pyr_2en)FeCl and of 6.20×10^{-3} M for (pyr_2en)MnCl.

Optical Properties. Both (pyr_2en)FeCl and (pyr_2en)MnCl were characterized via UV−vis and fluorescence spectroscopy in Milli-Q water solution. The electronic absorption spectra of **1** and **2** exhibited three main absorption bands in the range between 200 and 350 nm and a less intense band at higher wavelengths. These bands were also found in the spectrum of the free ligand pyr_2enH_2 and can therefore be assigned to $\pi \rightarrow$

dx.doi.org/10.1021/ic401055k | *Inorg. Chem.* 2013, 52, 11778−11786

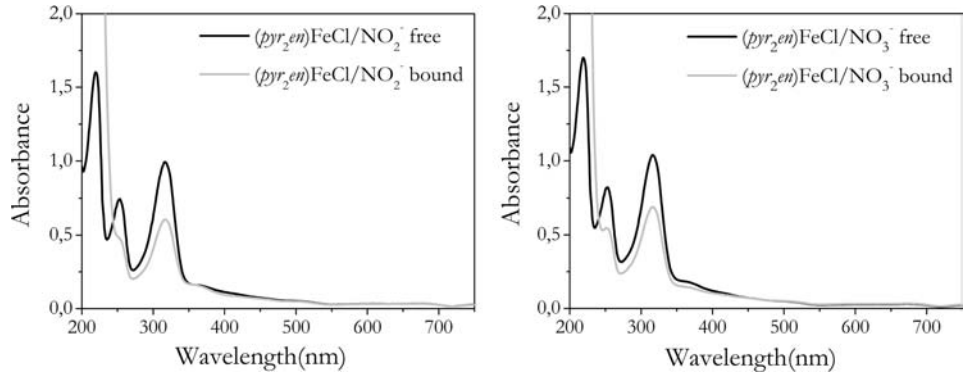

Figure 2. Electronic absorption spectra of (pyr_2en)FeCl upon addition of an excess of $NaNO_2$ or $NaNO_3$ (rt, 50 μM, MQ water).

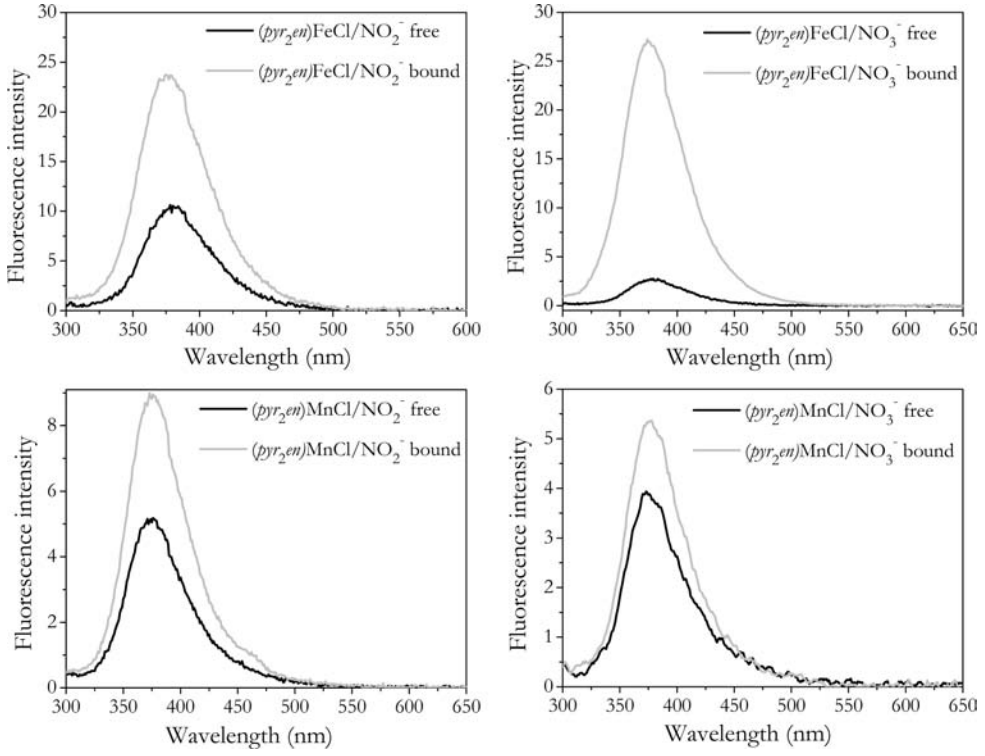

Figure 3. Emission spectra of (pyr_2en)FeCl or (pyr_2en)MnCl (exc 274 nm) upon addition of an excess of $NaNO_2$ or $NaNO_3$ (rt, 50 μM, MQ water).

π^* intraligand transitions[32,33] (see Supporting Information). Both the complexes **1** and **2** were slightly fluorescent and exhibited an emission band in the near-UV region (around 380 nm) (Figures S4 and S5 in the Supporting Information). When exciting an aqueous solution of the free ligand, under the same experimental conditions, an higher emission of fluorescence was observed (Figures S6 and S7 in the Supporting Information). Thus metal coordination induces a consistent quenching of the fluorescence of the free pyr_2en ligand.

Nitrite and Nitrate Response of 1 and 2. Interactions between (pyr_2en)FeCl or (pyr_2en)MnCl and NO_3^- or NO_2^- were studied by UV−vis and fluorescence spectroscopy. In the first instance, we tested the aptness of **1** or **2** to act as NO_2^- and NO_3^- recognition elements by UV−vis spectroscopy. Figure 2 shows the spectral changes observed after addition of NO_3^- or NO_2^-. When an excess of NO_3^- or NO_2^- was added to a Milli-Q solution of **1** or **2** a hyperchromic shift in the absorption spectra was observed indicating that the NO_3^- and NO_2^- effectively cause some perturbation in the electronic structure of complexes **1** and **2**. Although the spectral changes for **1** were evident (see Figure 2), the increase in absorption for **2** was not very significant (Figures S10 and S11 in the Supporting Information).

More pronounced changes were observed in the fluorescence responses of **1** and **2** toward NO_2^- or NO_3^- anions (Figure 3). Addition of NO_2^- or NO_3^- to a Milli-Q solution of **1** or **2** resulted in consistent enhancements of the fluorescence intensity giving rise to the OFF−ON fluorescent response in all the cases.[34]

When increasing amounts of NO_3^- or NO_2^- were added and the fluorescence intensities were monitored, a progressive enhancement was observed. In all cases, when the fluorescence intensity values were plotted against the NO_2^- and NO_3^- concentrations, typical saturation binding curves were observed. As an example, Figure 4 shows the NO_3^- titration of (pyr_2en)FeCl. The changes in the emission spectra were fitted

dx.doi.org/10.1021/ic401055k | Inorg. Chem. 2013, 52, 11778−11786

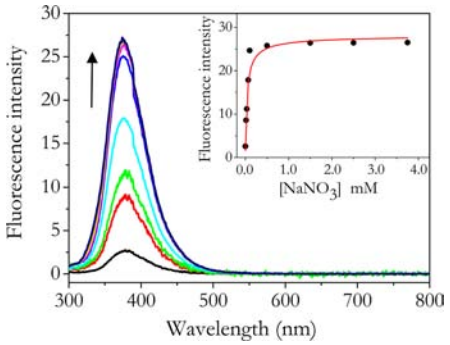

Figure 4. Emission spectra of (pyr_2en)FeCl (exc 274 nm) when titrated with $NaNO_3$ ([**1**] = 50 μM, rt, MQ water).

to 1:1 binding isotherms. For (pyr_2en)FeCl, the values of apparent equilibrium constants of association (K_a) were found to be 3.0×10^5 and 2.8×10^5 M^{-1} for NO_2^- and NO_3^-, respectively. For (pyr_2en)MnCl, the values of K_a were 8.7×10^2 and 8.3×10^3 M^{-1} for NO_2^- and NO_3^-, respectively. The association constants for the Mn complex are quite low, this could preclude practical applications for this complex. The association constants for the Fe complex are higher than those reported for much more elaborate receptors that bind nitrite or nitrate anion via multiple hydrogen bonds.[35] Very few examples of coordination compounds able to achieve nitrogen oxyanion binding have been reported so far. Recently, a tetraphenyl porphyrin zinc complex was utilized for nitrite and nitrate recognition, resulting in an efficient receptor for the these anions in 70% 2-propanol/water (v/v) solution.[19] In our case, the binding experiments were carried out in water, and a strong interaction was observed. Their implications for nitrite and nitrate sensing in water are thus very promising.

Selectivity. To obtain an indication of the selectivity of the devised constructs, we selected the better performing of our constructs (complex **1**) and checked its fluorescence intensity in the presence of biologically relevant and potentially competing anions (i.e., CH_3COO^-, F^-, HPO_4^{2-}, $C_3H_5O(COO)_3^{3-}$, $C_2O_4^{2-}$, HCO_3^-). In the presence of each one of the above-mentioned anions, the fluorescence intensity of **1** stayed mostly unchanged, thus suggesting high selectivity of our probe in the experimental conditions tested (see Figure 5). In the same experimental conditions, addition of NO_3^- leads to an increase of about 90% in emission intensity. Nitrite provokes a lower turn-on signal; it is of about 25% of that observed for nitrate. So the response is quite selective for nitrate over nitrite and other relevant anions.

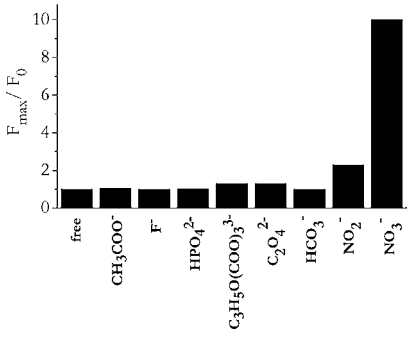

Figure 5. Relative fluorescence emission at 375 nm (λ_{ex}= 274 nm) of complex **1** (50 μM) in the presence of CH_3COONa, NaF, Na_2HPO_4, $Na_3C_3H_5O(COO)_3$, $Na_2C_2O_4$, $NaHCO_3$, $NaNO_2$, or $NaNO_3$ (500 μM each) in aqueous solution.

Investigation into the Recognition Mechanism of NO_3^- and NO_2^-. One of the three following different scenarios may describe the mechanism by which NO_3^- and NO_2^- induce a fluorescence response upon their addition to the aqueous solution of complexes **1** and **2**: (i) the excess of anion could extract the metal from the complex causing the release of the organic ligand; (ii) the metal complexes **1** and **2** have an axial coordination site, so the recognition of nitrite or nitrate could occur through the coordination of the anion to the metal center; (iii) the binding of the nitrite or nitrate anion could occur through the displacement of the chloride anion.

We focused on studying the reaction between complex **1** and NO_3^-. At first, we analyzed the ^{1}H NMR spectrum of complex **1** in the presence of excess of nitrate anion. No significant change in the initial ^{1}H NMR spectrum was observed upon addition of nitrate to a D_2O solution of **1** (see Figure S19 in Supporting Information). This finding excludes scenario i since in that case when nitrate was added the spectrum of the starting ligand should have become detectable. To assess whether the reaction occurring is that in ii or in iii, we examined the reaction between complex **1** and NO_3^- by electrospray ionization mass spectrometry. When the ESI spectrum of the reaction mixture between complex **1** and an excess of NO_3^- was measured soon after the mixing, this results in two predominant peaks at 448.2 and 475.2 m/z (see Figure 6). These peaks were attributed to

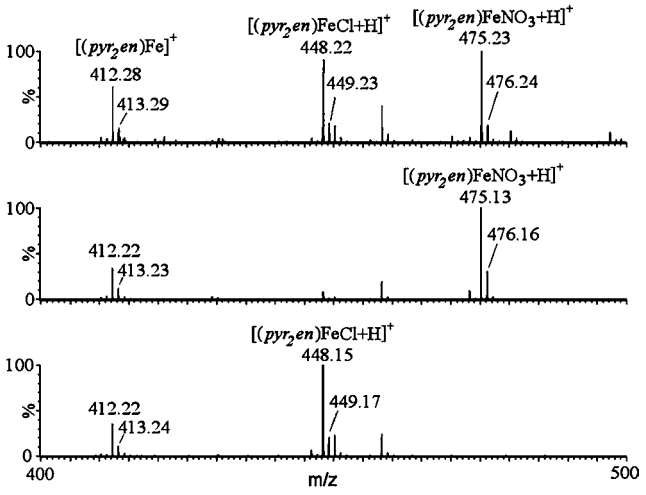

Figure 6. ESI mass spectra of aqueous solutions containing **1** (bottom), **4** (middle), and **1** + 10 equiv of $NaNO_3$ (top).

the species [(pyr_2en)FeCl + H]$^+$ and [(pyr_2en)$FeNO_3$ + H], respectively. The first peak was already evident in the ESI spectrum of complex **1**, the second in that of complex **4** (vide infra). No peaks could be detected when the ESI spectrum of the reaction mixture was measured in the negative mode. These findings provide clear evidence for scenario iii. Literature data on manganese Schiff base complexes also support the anion-exchange reaction mechanism (scenario iii).[36]

Nitrite and Nitrate Coordination: X-ray Structures of Manganese NO_2^- and NO_3^- Adducts. Nitrite and nitrate anions may be bound terminally to a single metal atom or bridging to two or more metal atoms.[37−39] In the terminal coordination mode, nitrite anion can be coordinated via the nitrogen atom (nitro case) or via one or two oxygen atoms (nitrito case) (Scheme 2).

dx.doi.org/10.1021/ic401055k | Inorg. Chem. 2013, 52, 11778−11786

Scheme 2

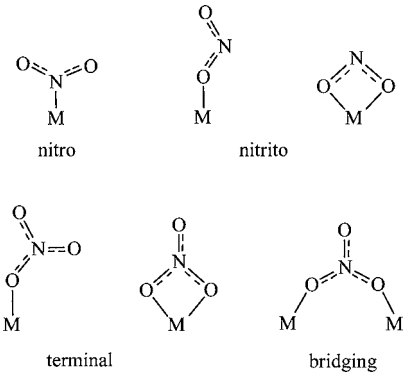

In order to gain more insight in the binding mode of nitrite and nitrate anions to the metal center of our pyridoxal base complexes, the corresponding NO_2^- or NO_3^- adducts were isolated on a preparative scale. The synthesis of the nitrite complex $(pyr_2en)FeNO_2$ (**3**) was achieved by an anion exchange reaction of the in situ formed $(pyr_2en)Fe(OAc)$ with an excess of $NaNO_2$. The nitrate complex $(pyr_2en)FeNO_3$ (**4**) was obtained by the direct treatment of pyr_2en^{2-} with 1 equiv of $Fe(NO_3)_3$ in methanol at room temperature. Despite several attempts, we could not obtain single crystals of complexes **3** and **4** suitable for X-ray structure analysis.

Nitrito and nitrate manganese(III) complexes, $(pyr_2en)MnNO_2$ (**5**) and $(pyr_2en)MnNO_3$ (**6**), were obtained in good yield by reacting the deprotonated ligand with 1 equiv of $Mn(OAc)_2{\cdot}4H_2O$ in air. The acetate ligand was replaced upon addition of an excess of $NaNO_2$ or $NaNO_3$ to the reaction mixtures. Slow cooling of saturated methanol solutions yielded single crystals suitable for X-ray diffraction. Figures 7 and 8

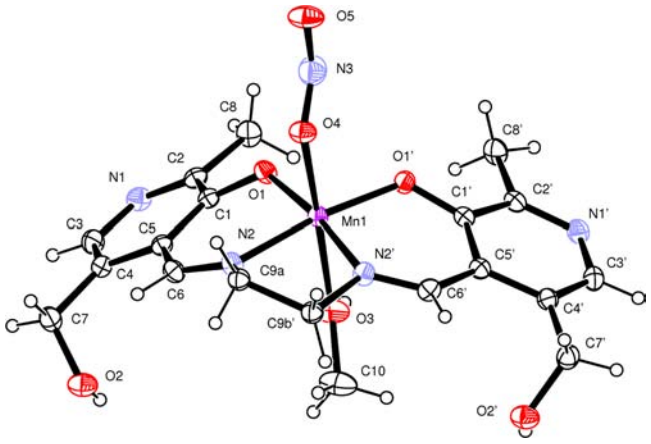

Figure 7. An ORTEP view of compound $(pyr_2en)MnNO_2$ (**5**) showing the thermal ellipsoids at 30% probability level.

display the ORTEP[40] views of $(pyr_2en)MnNO_2$ and $(pyr_2en)MnNO_3$. A selection of bond distances and angles are given in Tables S3 and S4 of Supporting Information. Both complexes display a distorted octahedral coordination where the Mn is bonded, in the equatorial plane, to four atoms (N_2O_2) of the pyr_2en ligand. In $(pyr_2en)MnNO_2$ (**5**), the apical positions are occupied by a nitrite anion, coordinated in a monodentate fashion, and a methanol molecule bound through oxygen atoms. In $(pyr_2en)MnNO_3$ (**6**), the axial position consists of a

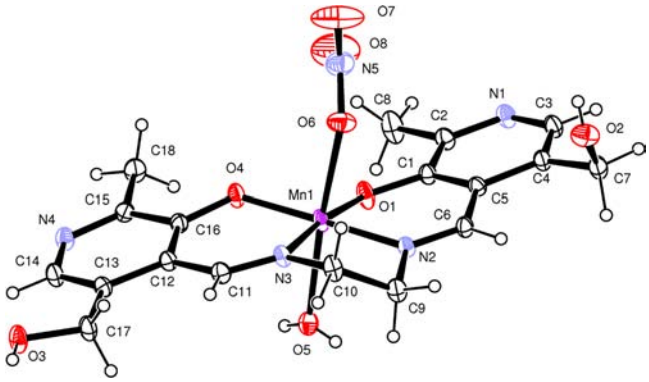

Figure 8. An ORTEP view of compound $(pyr_2en)MnNO_3$ (**6**) showing the thermal ellipsoids at 30% probability level.

nitrate anion, coordinated with an oxygen atom to Mn and a water molecule.

In both compounds, the bond distances and angles in the $Mn(N_2O_2)$ units are normal for an octahedral Mn(III) Schiff base complex (Tables S3 and S4, Supporting Information) and the elongation of Mn−O axial distances, in the range 2.160(2)−2.298(3) Å, can be accounted for Jahn−Teller effect.[41−44] In $(pyr_2en)MnNO_2$ (**5**), the two O−N bonds of the nitrito ligands are statistically equivalent [1.244(4) and 1.245(4) Å], while in other nitrito anions coordinated to Mn(III), the O−N bonds are not equal, the longest bond being formed by the coordinated oxygen.[45,46] The ligand is bent with an ONO angle of 126.9(4)°. The hydrogen bond scheme in the crystal of **5** (see Supporting Information, Figure S21) displays a chainlike structure running parallel to the *a* axis, where the methanol O3H group is linked to the O5 nitrite oxygen by means of a strong O3−H···O5 hydrogen bond [O3···O5 = 2.659(3) Å]. The other intermolecular O2−H2···N1 hydrogen bond links the molecules in corrugated tapes perpendicular to the previous chain. In the $(pyr_2en)MnNO_2$ (**5**) complex, the N−O bond distances of the coordinated nitrate anion are not equivalent, the longest N−O bond of 1.252(3) Å corresponding to that involving the coordinated oxygen, as observed for other structures of Mn(III).[42,43,45] The crystal packing (see Supporting Information, Figure S21) is dominated by an extended hydrogen bond network built up by the intermolecular interactions among the hydroxy O3−H and O2−H groups, the pyridine N1 and N4 nitrogens, the oxygens of the nitrate anion, and the water molecule.

Quantum Chemical Calculations on Anion Binding. In order to qualitatively understand the binding affinity of the nitrogen oxyanions NO_2^- and NO_3^- toward the iron and manganese complexes, density functional calculations (DFT) were undertaken. In our calculations, the metal center was considered in an octahedral coordination environment with the pyr_2en ligand in the equatorial plane, and water and nitrite, or nitrate, or chloride anion in the two additional apical positions. To save computational resources, the pyr_2en ligand was mimicked by a truncated model comprising only the conjugated core and missing the two aromatic rings, this model was frequently used for theoretical studies of metal−salen complexes.[47]

As shown above, it is reasonable to assume that the binding of nitrite or nitrate anion occurs through the coordination of the anion to the metal center according to the following reaction:

dx.doi.org/10.1021/ic401055k | *Inorg. Chem.* 2013, 52, 11778−11786

$$(pyr_2en)MCl(H_2O) + NO_x^- \rightarrow (pyr_2en)MNO_x(H_2O) + Cl^- \quad (1)$$

For both complexes (M = Fe or Mn), the substitution of the chloride anion by the nitrite or nitrate anion is predicted to be exergonic (see Supporting Information). The displacement by the nitrite anion is expected to be more favored than the displacement by the nitrate anion for both complexes. As an example, in the case of the iron complex, the calculated Gibbs free energy change (ΔG) for the substitution of the chloride with the nitrite is -16.4 kcal·mol^{-1}, whereas the substitution of the chloride anion with the nitrate anion is -2.0 kcal·mol^{-1}. An important contribution to these reactions is given by the energies of hydration. As matter of fact, the chloride anion has an higher hydration than nitrite or nitrate anion, so the displacement of chloride lead to a gain in the hydration energy favoring the reaction. In order to roughly estimate the solvation effect, we compared the computed ΔG values obtained in water with the computed ΔG values obtained in gas phase ($\Delta\Delta G = \Delta G_{H_2O} - \Delta G_{gas}$). For the iron complex, the $\Delta\Delta G$ is -5.8 and -10.6 kcal·mol^{-1} for the displacement by nitrite and nitrate, respectively. In the case of the manganese complex, the $\Delta\Delta G$ is -5.7 and -10.4 kcal·mol^{-1} for the displacement by nitrite and nitrate, respectively. The higher gain in the hydration energy obtained for the nitrate substitution is corroborated by the difference in the experimental free energy of hydration of chloride[48] ($\Delta G_{hyd}(Cl^-) = -89.6$ kcal·mol^{-1}), nitrite[48] ($\Delta G_{hyd}(NO_2^-) = -81.0$ kcal·mol^{-1}), and nitrate[48] ($\Delta G_{hyd}(NO_3^-) = -73.1$ kcal·mol^{-1}). It is worth noting that in the case of the nitrate substitutions, the gain in the hydration energy seems to be the driving force for the reactions. Even though the NO_3 adducts $(pyr_2en)MNO_3^-(H_2O)$ are predicted to be stable, their formations, starting from the Cl adducts, are not favored: in gas phase, these reactions are predicted to be slightly endergonic by 8.6 and 9.7 kcal·mol^{-1} for **1** and **2**, respectively.

The differences in hydration energy seem to be the origin of the selectivity of our complexes. As matter of fact, the free energy of hydration of the competitive anions tested in this work are lower (more negative) than that of chloride anion.[48] In these cases, the substitution of chloride anion would lead to a loss in the hydration energy.

CONCLUSIONS

New water-soluble iron(III) and manganese(III) metal complexes bearing a pyridoxal-based salen ligand have been synthesized and characterized. Their aptness to act as receptors for nitrite and nitrate anions in water solutions has been explored. The possibility of performing the measurements in aqueous solution represents an advantage for our system. High hydration energy, large ionic radii, and weak basicity of nitrite and nitrate anions make particularly challenging the development of effective and selective receptors for these anions, especially in an aqueous solution. Literature features only a few examples of artificial receptors that are capable of recognizing nitrite or nitrate in neutral aqueous or aqueous/organic solution. Our experiments show that complex **1** can be successfully implemented as a nitrate and nitrite fluorescent probe in aqueous solutions. Indeed, addition of NO_2^- or NO_3^- to a Milli-Q solution of **1** or **2** induced consistent enhancements of the fluorescence intensity giving rise to a turn-ON fluorescence response in all the cases. In the case of complex **1**, high binding constants and good selectivity were obtained for the nitrate recognition. It was shown that the addition of nitrite or nitrate results in chloride displacement, causing an increase in fluorescence emission. The corresponding NO_2^- or NO_3^- adducts were isolated on a preparative scale. In the case of manganese, the X-ray structures of both the adducts were successfully resolved.

A limitation of our systems is the fact that they make use of UV excitation. This is more or less true for any sensor and any wavelength, but the more the dye absorbs to the UV the more there is the chance to excite other compounds. The higher fluorescence switching of the receptor upon analyte binding, the more selective will be the fluorescence signal. For instance, in the case of complex **1** the high fluorescence switching upon nitrite and above all nitrate binding partly compensates for the disadvantage of using UV excitation and allows for eventual corrections. Further research is underway to improve our sensors in this respect by screening for other ligands with better properties (absorption at longer wavelength and possibly higher quantum yield).

The present data provide proof-of-principle that it is possible to monitor weak coordinating anions by using metal based coordination complexes. Efforts to increase and optimize sensitivity so as to combine our systems with immobilization techniques are underway.

EXPERIMENTAL SECTION

Materials. All chemicals used for the synthetic work were obtained from Sigma-Aldrich or Strem Chemicals and were of reagent grade. They were used without further purification. The ligand pyr_2enH_2 (pyr_2enH_2 = *N*,*N*′-ethylenebis(pyridoxylideneiminato)) was prepared as previously reported.[49]

Elemental analyses were performed with a PERKIN-Elmer 240-C. Mass spectrometry analyses were carried out using a Micromass Quattro micro API triple quadrupole mass spectrometer equipped with an electrospray ion source (Waters, Milford, MA). Room temperature NMR spectra were recorded on a Bruker AVANCE 400 NMR instrument (^{1}H, 400.13 MHz; ^{13}C, 100.62 MHz).

Synthesis of $(pyr_2en)FeCl$ (1). Ligand pyr_2enH_2 (0.200 g, 0.558 mmol) was dissolved in methanol (10 mL), and NaOEt was added as solid (0.076 g, 1.12 mmol). The bright yellow reaction mixture was left under stirring for 1 h. $FeCl_3$ (0.090 g, 0.558 mmol) dissolved in methanol (5 mL) was slowly added, and the reaction mixture became dark. The reaction was left under stirring overnight. A brown-red solid was collected by filtration, washed with methanol and diethyl ether, and dried under vacuum. Yield: 0.137 g, 49%. $C_{18}H_{20}N_4O_4FeCl\cdot CH_3OH$: calcd. C 47.57, H 5.04, N 11.68; found C 47.30, H 4.96, N 11.83. MS (ESI acetonitrile): *m*/*z* (%) 412.2 (40) $[(pyr_2en)Fe]^+$, 448.15 (100) $[(pyr_2en)FeCl + H]^+$, 458.19 (25) $[(pyr_2en)Fe + HCO_2H]^+$. Selected IR (KBr, cm^{-1}): 1626(s), 1501-(m),1398(s),1377(s), 1313(s), 1263(m), 1201(m), 1038(m), 764(m), 741(m), 621(s), 454(m). Emission (H_2O, λ_{exc} = 274 nm), λ_{max} (quantum yield,Φ_F): 377 nm (0.004).

Synthesis of $(pyr_2en)MnCl$ (2). Ligand pyr_2enH_2 (0.255 g, 0.711 mmol) was dissolved in methanol (10 mL), and NaOEt was added as solid (0.097 g, 1.42 mmol). The bright yellow reaction mixture was left under stirring for 1 h. $Mn(CH_3COO)_2\cdot 4H_2O$ (0.174 g, 0.711 mmol) dissolved in methanol (5 mL) was slowly added, and the reaction mixture became dark brown. The reaction mixture was left under stirring overnight. The day after an excess of NaCl (5:1 molar ratio respect to the manganese) was added as a 0.6 M aqueous solution. The resulting dark brown solution was left at −20 °C overnight. A brown solid was collected by filtration, washed with methanol and diethyl ether, and dried under vacuum. Yield: 0.283 g, 83%. $C_{18}H_{20}N_4O_4MnCl\cdot CH_3OH$: calcd. C 47.66, H 5.05, N 11.70; found C 47.40, H 4.93, N 11.86. MS (ESI acetonitrile): *m*/*z* (%) 410.9 (100) $[(pyr_2en)Mn]^+$, 446.9 (10) $[(pyr_2en)MnCl + H]^+$, 452.0 (10)

dx.doi.org/10.1021/ic401055k | Inorg. Chem. 2013, 52, 11778−11786

$[(pyr_2en)Mn+CH_3CN]^+$. Selected IR (KBr, cm^{-1}): 1616(s), 1438(m), 1390(s), 1306(m), 1260(s), 1191(m), 1042(m), 909(m), 766(m), 744(m), 627(s), 489(m). Emission (H_2O, λ_{exc} = 274 nm), λ_{max} (quantum yield,Φ_F): 376 nm (0.001).

Synthesis of $(pyr_2en)FeNO_2$ (3). Ligand pyr_2enH_2 (0.200 g, 0.558 mmol) was dissolved in methanol (10 mL), and NaOEt was added as solid (0.076 g, 1.12 mmol). The bright yellow reaction mixture was left under stirring for 1 h. $Fe(CH_3COO)_3$ (0.130 g, 0.558 mmol) dissolved in methanol (5 mL) was slowly added, and the reaction mixture became dark brown. The reaction mixture was left under stirring overnight. The day after an excess of $NaNO_2$ (5:1 molar ratio respect to the iron) was added as a 0.6 M aqueous solution. The resulting dark red solution was left at −20 °C overnight. A red solid was collected by filtration, washed with methanol and diethyl ether, and dried under vacuum. Yield: 0.200 g, 73%. $C_{18}H_{20}N_5O_6Fe{\cdot}CH_3OH$: calcd. C 46.55, H 4.93, N 14.28; found C 46.82, H 4.89, N 14.86. Selected IR (KBr, cm^{-1}): 1620(s), 1406(s), 1395(s), 1311(m), 1265(m), 1200(m), 1039(m), 624(m), 457(m). Emission (H_2O, λ_{exc} = 274 nm), λ_{max} (quantum yield,Φ_F): 375 nm (0.010).

Synthesis of $(pyr_2en)FeNO_3$ (4). Ligand pyr_2enH_2 (0.200 g, 0.558 mmol) was dissolved in methanol (10 mL), and NaOEt was added as solid (0.076 g, 1.12 mmol). The bright yellow reaction mixture was left under stirring for 1 h. $Fe(NO_3)_2{\cdot}9H_2O$ (0.225 g, 0.558 mmol) dissolved in methanol (5 mL) was slowly added, and the reaction mixture became dark red. The reaction mixture was left under stirring overnight. A dark red solid was collected by filtration, washed with methanol and diethyl ether, and dried under vacuum. Yield: 0.180 g, 64%. $C_{18}H_{20}N_5O_7Fe{\cdot}CH_3OH$: calcd. C 45.08, H 4.78, N 13.83; found C 45.70, H 4.86, N 13.96. MS (ESI acetonitrile): m/z (%) 412.2 (40) $[(pyr_2en)Fe]^+$.475.13 (100) $[(pyr_2en)FeNO_3 + H]^+$.Selected IR (KBr, cm^{-1}): 1637(s), 1497(s), 1384(vs), 1319(s), 1205(m), 1045(m), 825(m), 753(m), 617(m). Emission (H_2O, λ_{exc} = 274 nm), λ_{max} (quantum yield,Φ_F): 375 nm (0.025).

Synthesis of $(pyr_2en)MnNO_2$ (5). Ligand pyr_2enH_2 (0.200 g, 0.558 mmol) was dissolved in methanol (10 mL), and NaOEt was added as solid (0.076 g, 1.12 mmol). The bright yellow reaction mixture was left under stirring for 1 h. $Mn(CH_3COO)_2{\cdot}4H_2O$ (0.137 g, 0.558 mmol) dissolved in methanol (5 mL) was slowly added, and the reaction mixture became dark brown. The reaction mixture was left under stirring overnight. The day after an excess of $NaNO_2$ (5:1 molar ratio respect to the manganese) was added as a 0.6 M aqueous solution. The resulting dark brown solution was left at −20 °C overnight. A brown solid was collected by filtration, washed with methanol and diethyl ether, and dried under vacuum. Yield: 0.131 g, 48%. $C_{18}H_{20}N_5O_6Mn{\cdot}CH_3OH$: calcd. C 46.63, H 4.94, N 14.31; found C 46.70, H 4.87, N 14.56. Emission (H_2O, λ_{exc} = 274 nm), λ_{max} (quantum yield,Φ_F): 374 nm (0.002).

Synthesis of $(pyr_2en)MnNO_3$ (6). Ligand pyr_2enH_2 (0.200 g, 0.558 mmol) was dissolved in methanol (10 mL), and NaOEt was added as solid (0.076 g, 1.12 mmol). The bright yellow reaction mixture was left under stirring for 1 h. $Mn(CH_3COO)_2{\cdot}4H_20$ (0.137 g, 0.558 mmol) dissolved in methanol (5 mL) was slowly added, and the reaction mixture became dark brown. The reaction mixture was left under stirring overnight. The day after an excess of $NaNO_3$ (5:1 molar ratio respect to the manganese) was added as a 0.6 M aqueous solution. The resulting dark brown solution was left at −20 °C overnight. A brown solid was collected by filtration, washed with methanol and diethyl ether, and dried under vacuum. Yield: 0.122 g, 44%. $C_{18}H_{20}N_5O_7Mn{\cdot}H_2O$: calcd. C 44.00, H 4.51, N 14.25; found C 43.84, H 4.78, N 14.63. Emission (H_2O, λ_{exc} = 274 nm), λ_{max} nm (quantum yield,Φ_F): 374 nm (0.001).

Absorbance and Fluorescence Measurements. Absorption spectra were recorded on a Cary-50 spectrophotometer, using a 1 cm quartz cuvette (Hellma Benelux bv, Rijswijk, Netherlands) and a slit-width equivalent to a bandwidth of 5 nm. Fluorescence spectra were measured on a Cary Eclipse spectrophotometer in a 10 × 10 mm^2 airtight quartz fluorescence cuvette (Hellma Benelux bv, Rijswijk, Netherlands) with an emission band-pass of 10 nm and an excitation band-pass of 5 nm. Both absorption and fluorescence measurements were performed in Milli-Q water at room temperature. Fluorescence experiments were performed with excitation at 274 nm. The 274 nm excitation wavelength was selected because both free $NaNO_2$ and free $NaNO_3$ have only little absorption at this wavelength.

Fluorescence quantum yield (Φ_F) values were measured in optically diluted solutions using phenol (Φ_F = 0.014 in Milli-Q water) as standard, according to the according to the equation:[50]

$$\Phi_F^s = \Phi_F^r(I_s/I_r)(A_r/A_s)(\eta_s/\eta_r)^2$$

where indexes s and r denote the sample and reference, respectively. I stands for the integrated emission intensity, A is the absorbance at the excitation wavelength, and η is the refractive index of the solvent.

Titration Experiments. These experiments were performed as follows: the cuvette was filled with sample solutions in Milli-Q water solution. Then microliter amounts of $NaNO_2$ (or $NaNO_3$) solutions in Milli-Q water (to the end concentrations specified in the figure captions) were injected via a gastight syringe. Spectra were registered when the fluorescence reached the threshold value, which corresponds to the saturation point in the present case.

The changes in the emission spectra were fitted using the following equation:

$$F_{NO_x} = F_0 - \{(F_0 - F_\infty)[NO_x]\}/\{[NO_x] + K_d\}$$

where NO_x is the concentration of free NO_2^- or NO_3^- in solution and F_0 and F_∞ denote the emission intensities of the NO_x-free and NO_x-bound $(pyr_2en)FeCl$ or $(pyr_2en)MnCl$, respectively.

ESI MS Experiments. ESI experiments were performed in H_2O/CH_3CN (50:50) with 0.5% formic acid. For the in situ experiments between complex **1** and $NaNO_3$, the reaction was performed in Milli-Q water in a 1:10 molar ratio, and then an aliquot of the mixture was diluted in H_2O/CH_3CN (50:50) with 0.5% formic acid.

Computational Details. Molecular structures and electronic energies for all molecules discussed here were calculated using the Gaussian 09[51] packages. All geometries were optimized without constraints at the BP86 level of theory, that is, by employing the exchange and correlation functionals of Becke[52] and Perdew,[53,54] respectively. The basis set consisted of the Los Alamos basis sets and corresponding effective core potentials of Hay and Wadt[55,56] (LANL2DZ) for Fe and Mn and of the 6-31G(d) basis sets for all other atoms. A tight gradient convergence criterion with ultrafine integration grid was specified in these calculations. No constraints were imposed during the optimizations. Stationary point geometries were characterized as local minimum on the potential energy surfaces. The absence of imaginary frequency demonstrated that structures were true minima at their respective levels of theory.

The Fe^{3+} and Mn^{3+} ions have the [Ar] $3d^5$ and [Ar] $3d^4$ electron configurations, respectively. As a result, $(pyr_2en)Fe$ and $(pyr_2en)Mn$ have three different spin states (Fe^{3+}, S = 1/2, 3/2, 5/2; Mn^{3+}, S = 0, 1, 2). Calculated relative energies of the $(pyr_2en)Fe(H_2O)X$ and $(pyr_2en)Mn(H_2O)X$ ($X = Cl^-$, NO_2^-, NO_3^-) are summarized in Table S5, Supporting Information. According to our calculations, the lowest-energy structures of the model complexes $(pyr_2en)Fe(H_2O)X$ correspond to the low-spin states (S = 1/2). For example, the low-spin state of the $(pyr_2en)Fe(H_2O)Cl$ is more stable than the high-spin states (S = 3/2, 5/2) by 6.9 and 13.4 kcal/mol, respectively. The low-spin state was assumed for all the Fe(III) species considered in this work. In the case of Mn complexes, the triplet states (S = 1) lie very close in energy to the quintuplet states (S = 2). For the model complex $(pyr_2en)Mn(H_2O)Cl$, the triplet state lies 0.1 kcal/mol below the quintuplet state. In the case of nitrite and nitrate Mn complexes, the calculations on triplet states gave reasonable ground-state descriptions; on the contrary the geometry optimizations on quintuplet state resulted in energy minimized structures with strong structural rearrangements. For this reason, the triplet state (S = 3) was assumed for all the Mn(III) species considered in this work.

Solvent effects (water) have been estimated in single-point calculations on the gas phase optimized structures based on the polarizable continuous solvation model, PCM,[57] as implemented in Gaussian 09. The gas-phase energies were corrected by the solvation term.

The Gibbs free energy change (ΔG, thermodynamically corrected to 298 K) were calculated using eq 2:

$$\Delta G = [G((pyr_2en)M(H_2O)NO_x + G(Cl^-)] - [G((pyr_2en)M(H_2O)Cl + G(NO_x)] \quad (2)$$

Cartesian coordinates of all DFT optimized structures are available on request.

Crystal Structure Determinations. The crystal data of compounds $(pyr_2en)FeCl$ (**1**), $(pyr_2en)MnNO_2$ (**5**), and $(pyr_2en)MnNO_3$ (**6**) were collected at room temperature using a Nonius Kappa CCD diffractometer with graphite monochromated Mo Kα radiation. The data sets were integrated with the Denzo-SMN package[58] and corrected for Lorentz, polarization, and absorption effects (SORTAV).[59] The structures were solved by direct methods using the SIR97[60] system of programs and refined using full-matrix least-squares with all non-hydrogen atoms anisotropically and hydrogens included on calculated positions, riding on their carrier atoms, except for compounds **5** and **6**, the hydrogens involved in hydrogen bonds, which were refined isotropically.

The structure of **1** displays some disorder, and the hydrogen atoms for the hydroxyl groups and water molecules could not be localized.

The structure of $(pyr_2en)MnNO_2$ (**5**) is located on a crystallographic mirror plane passing through Mn1, the nitrite anion, and O3 oxygen of the methylic alcohol. Accordingly, $C9aH_2$, $C9bH_2$, and $C10H_3$ groups are disordered and refined with occupancy of 0.5 each.

All calculations were performed using SHELXL-97[61] and PARST[62] implemented in WINGX[63] system of programs.

Crystal Data. Complex **1** $(C_{18}H_{23}ClFeN_4O_5)^+\cdot Cl^-\cdot 3H_2O$; triclinic, space group $P1$, a = 8.8332(2), b = 9.9439(2), c = 13.8786(3) Å, α = 78.2203(8)°, β = 76.8323(8)°, γ = 84.2275(10)°, V = 1160.13(4) Å^3, Z = 2, D_c = 1.592 g cm^{-3}. Intensity data collected with $\theta \leq 28.0°$; 5578 independent reflections measured; 4762 reflections observed [$I > 2\sigma(I)$]. Final R = 0.0609 (observed reflections), and R_w = 0.2010 (all reflections); no. of parameters = 598; GOF = 1.072.

Complex **5** $C_{19}H_{24}MnN_5O_7$; monoclinic, space group $P2_1/m$, a = 7.7911(2), b = 17.2678(5), c = 8.2311(3) Å, β = 108.603(2)°, V = 1049.51(6) Å^3, Z = 2, D_c = 1.549 g cm^{-3}. Intensity data collected with $\theta \leq 27.85°$; 2563 independent reflections measured; 1934 reflections observed [$I > 2\sigma(I)$]. Final R = 0.0423 (observed reflections), and R_w = 0.1152 (all reflections); no. of parameters = 163; GOF = 1.048.

Compound **6** $C_{18}H_{22}MnN_5O_8$; triclinic, space group $P\bar{1}$, a = 8.7425(2), b = 8.7874(2), c = 14.5986(5) Å, α = 80.070(1)°, β = 74.306(1)°, γ = 71.557(2)°, V = 1019.61(5) Å^3, Z = 2, D_c = 1.600 g cm^{-3}. Intensity data collected with $\theta \leq 27.50°$; 4635 independent reflections measured; 3529 reflections observed [$I > 2\sigma(I)$]. Final R = 0.0434 (observed reflections), and R_w = 0.1147 (all reflections), no. of parameters = 307; GOF = 1.034.

Crystallographic data (excluding structure factors) have been deposited at the Cambridge Crystallographic Data Centre and allocated the deposition numbers CCDC 935854, $pyr_2enFeCl$ (**1**); 935855, $(pyr_2en)MnNO_2$ (**5**); 935856, $(pyr_2en)MnNO_3$ (**6**). These data can be obtained free of charge via www.ccdc.cam.ac.uk/conts/retrieving.html or on application to CCDC, Union Road, Cambridge, CB2 1EZ, UK [fax: (+44)1223-336033, e-mail: deposit@ccdc.cam.ac.uk].

■ ASSOCIATED CONTENT

Supporting Information

NMR spectra, absorption and fluorescence spectra, computational details, and X-ray crystallographic files (CIF). This material is available free of charge via the Internet at http://pubs.acs.org.

■ AUTHOR INFORMATION

Corresponding Author

*E-mail: smilione@unisa.it.

Notes

The authors declare no competing financial interest.

■ ACKNOWLEDGMENTS

The authors thank Dr. Maria Chiara Monti of the Department of Pharmacy (University of Salerno) for her help with ESI mass spectra, Dr. Tonino Caruso of the Department of Chemistry and Biology (University of Salerno) for his help with conductivity measurements, Dr. Silvia Sottini of the Department of Chemistry (University of Florence) for useful discussions, and Dr. Patrizia Iannece and Dr. Patrizia Oliva of the Department of Chemistry and Biology (University of Salerno) for their technical assistance.

■ REFERENCES

(1) Mitchell, H. H.; Shonle, H. A.; Grindley, H. S. *J. Biol. Chem.* **1916**, *24*, 461−490.
(2) Tannenbaum, S. R.; Correa, P. E. L. A. *Nature* **1985**, *317*, 675−676.
(3) Mensinga, T.; Speijers, G.; Meulenbelt, J. *Toxicol. Rev.* **2003**, *22*, 41−51.
(4) Butler, A. R.; Feelisch, M. *Circulation* **2008**, *117*, 2151−2159.
(5) Lundberg, J. O.; Weitzberg, E.; Gladwin, M. T. *Nat. Rev. Drug Discovery* **2008**, *7*, 156−167.
(6) Benjamin, N.; O'Driscoll, F.; Dougall, H.; Duncan, C.; Smith, L.; Golden, M.; McKenzie, H. *Nature* **1994**, *368*, 502.
(7) Kikuchi, K.; Nagano, T.; Hayakawa, H.; Hirata, Y.; Hirobe, M. *J. Biol. Chem.* **1993**, *268*, 23106−23110.
(8) Kotake, Y.; Tanigawa, T.; Tanigawa, M.; Ueno, I.; Allen, D. R.; Lai, C. S. *Biochim. Biophys. Acta* **1996**, *1289*, 362−368.
(9) Friedemann, M. N.; Robinson Scott, W.; Gerhardt Greg, A. *Anal. Chem.* **1996**, *68*, 2621−2628.
(10) Mao, L.; Shi, G.; Tian, Y.; Liu, H.; Jin, L.; Yamamoto, K.; Tao, S.; Jin, J. *Talanta* **1998**, *46*, 1547−1556.
(11) Moorcroft, M. J.; Davis, J.; Compton, R. G. *Talanta* **2001**, *54*, 785−803.
(12) Salimi, A.; Noorbakhash, A.; Karonian, F. S. *Int. J Electrochem. Sci.* **2006**, *1*, 435−445.
(13) Ito, K.; Takayama, Y.; Makabe, N.; Mitsui, R.; Hirokawa, T. *J. Chromatogr. A* **2005**, *1083*, 63−67.
(14) Ensafi, A. A.; Chamjangali, M. A. *Spectrochim. Acta A: Mol. Biomol. Spectrosc.* **2003**, *59*, 2897−2903.
(15) Martínez-Máñez, R.; Sancenón, F. *Chem. Rev.* **2003**, *103*, 4419−4476.
(16) Schmittel, M.; Lin, H. W. *Angew. Chem., Int. Ed.* **2007**, *46*, 893−896.
(17) Moragues, M. E.; Martinez-Manez, R.; Sancenon, F. *Chem. Soc. Rev.* **2011**, *40*, 2593−2643.
(18) Qinghai, S.; Bats, J. W.; Schmittel, M. *Inorg. Chem.* **2011**, *50*, 10531−10533.
(19) Whittington, C. L.; Maza, W. A.; Woodcock, H. L.; Larsen, R. W. *Inorg. Chem.* **2012**, *51*, 4756−4762.
(20) Sessler, J. R.; Gale, P. A.; Cho, W. S. *Anion Receptor Chemistry*; Royal Society of Chemistry: Cambridge, U.K.: 2006.
(21) Gale, P. A. *Acc. Chem. Res.* **2006**, *39*, 465−475.
(22) Schmidtchen, F. P. *Coord. Chem. Rev.* **2006**, *250*, 2918−2928.
(23) Strianese, M.; Palm, G. J.; Milione, S.; Kuhl, O.; Hinrichs, W.; Pellecchia, C. *Inorg. Chem.* **2012**, *51*, 11220−11222.
(24) Strianese, M.; Milione, S.; Bertolasi, V.; Pellecchia, C.; Grassi, A. *Inorg. Chem.* **2011**, *50*, 900−910.
(25) Strianese, M.; De Martino, F.; Pellecchia, C.; Ruggiero, G.; D'Auria, S. *Protein Pept. Lett.* **2011**, *18*, 282−286.
(26) Strianese, M.; Milione, S.; Maranzana, A.; Grassi, A.; Pellecchia, C. *Chem. Commun.* **2012**, *48*, 11419−11421.
(27) Boon, E. M.; Marletta, M. A. *J. Am. Chem. Soc.* **2006**, *128*, 10022−10023.

(28) Shyu, H. L.; Wei, H. H.; Lee, G. H.; Wang, Y. *J Chem. Soc., Dalton Trans.* **2000**, 915−918.
(29) Elmali, A.; Kavlakoglu, E.; Elerman, Y.; Svoboda, I., I *Acta Crystallogr.* **2000**, *C56* (Pt 9), 1097−1099.
(30) Dutta, S.; Biswas, P. *J. Mol. Struct.* **2011**, *996*, 31−37.
(31) Sarwar, M.; Madalan, A. M.; Lloret, F.; Julve, M.; Andruh, M. *Polyhedron* **2011**, *30*, 2414−2420.
(32) Bosnich, B. *J. Am. Chem. Soc.* **1968**, *90*, 627−632.
(33) Smith, H. E.; Neergaard, J. R.; Burrows, E. P.; Chen, F. M. *J. Am. Chem. Soc.* **1974**, *96*, 2908−2916.
(34) When a MilliQ water solution of complex **1**, **2**, or free ligand was excited, in the same experimental conditions, and the kinetic fluorescence spectrum was registered, no significant changes could be observed.
(35) Singh, A. S.; Sun, S. S. *J. Org. Chem.* **2012**, *77*, 1880−1890.
(36) Boucher, L. J.; Day, V. W. *Inorg. Chem.* **1977**, *16*, 1360−1367.
(37) Hitchman, M. A.; Rowbottom, G. L. *Coord. Chem. Rev.* **1982**, *42*, 55−132.
(38) Greenwood, N. N.; Earnshaw, A. *Chemistry of the Elements*, 2nd ed.; Butterworth-Heinemann: Oxford, U.K., 1993; Chapter 11.
(39) Morozov, I. V.; Serezhkin, V. N.; Troyanov, S. I. *Russ. Chem. Bull.* **2009**, *58*, 2407−2417.
(40) Burnett M. N.; Johnson C. K. Ortep-III: Oak Ridge Thermal Ellipsoid Plot Program for Crystal Structure Illustrations, 1996.
(41) Shyu, H. L.; Wei, H. H.; Wang, Y. *Inorg. Chim. Acta* **1999**, *290*, 8−13.
(42) Chen, C.; Huang, D.; Zhang, X.; Chen, F.; Zhu, H.; Liu, Q.; Zhang, C.; Liao, D.; Li, L.; Sun, L. *Inorg. Chem.* **2003**, *42*, 3540−3548.
(43) Darensbourg, D. J.; Frantz, E. B. *Inorg. Chem.* **2007**, *46*, 5967−5978.
(44) Kar, P.; Biswas, R.; Drew, M. G.; Ida, Y.; Ishida, T.; Ghosh, A. *Dalton Trans.* **2011**, *40*, 3295−3304.
(45) Suslick, K. S.; Watson, R. A. *Inorg. Chem.* **1991**, *30*, 912−919.
(46) Mossin, S.; Sørensen, H. O.; Weihe, H.; Glerup, J.; Søtofte, I. *Inorg. Chim. Acta* **2005**, *358*, 1096−1106.
(47) Takatani, T.; Sears, J. S.; Sherrill, C. D. *J. Phys.Chem. A* **2010**, *114*, 11714−11718.
(48) Custelcean, R.; Moyer, B. A. *Eur. J. Inorg. Chem.* **2007**, *2007*, 1321−1340.
(49) Correia, I.; Costa, P. J.; Duarte, M. T.; Henriques, R. T.; Piedade, M. F.; Veiros, L. F.; Jakusch, T.; Kiss, T.; Dornyei, A.; Castro, M. M.; Geraldes, C. F.; Avecilla, F. *Chem.—Eur. J.* **2004**, *10*, 2301−2317.
(50) Lakowicz, J. R. *Principles of Fluorescence Spectroscopy*; Kluwer Academic/Plenum: New York, Boston, Dordrecht, Moscow, 1996.
(51) Frisch, M. J.; Trucks, G. W.; Schlegel, H. B.; Scuseria, G. E.; Robb, M. A.; Cheeseman, J. R.; Montgomery, J. A., Jr.; Vreven, T.; Kudin, K. N.; Burant, J. C.; Millam, J. M.; Iyengar, S. S.; Tomasi, J.; Barone, V.; Mennucci, B.; Cossi, M.; Scalmani, G.; Rega, N.; Petersson, G. A.; Nakatsuji, H.; Hada, M.; Ehara, M.; Toyota, K.; Fukuda, R.; Hasegawa, J.; Ishida, M.; Nakajima, T.; Honda, Y.; Kitao, O.; Nakai, H.; Klene, M.; Li, X.; Knox, J. E.; Hratchian, H. P.; Cross, J. B.; Bakken, V.; Adamo, C.; Jaramillo, J.; Gomperts, R.; Stratmann, R. E.; Yazyev, O.; Austin, A. J.; Cammi, R.; Pomelli, C.; Ochterski, J. W.; Ayala, P. Y.; Morokuma, K.; Voth, G. A.; Salvador, P.; Dannenberg, J. J.; Zakrzewski, V. G.; Dapprich, S.; Daniels, A. D.; Strain, M. C.; Farkas, O.; Malick, D. K.; Rabuck, A. D.; Raghavachari, K.; Foresman, J. B.; Ortiz, J. V.; Cui, Q.; Baboul, A. G.; Clifford, S.; Cioslowski, J.; Stefanov, B. B.; Liu, G.; Liashenko, A.; Piskorz, P.; Komaromi, I.; Martin, R. L.; Fox, D. J.; Keith, T.; Al-Laham, M. A.; Peng, C. Y.; Nanayakkara, A.; Challacombe, M.; Gill, P. M. W.; Johnson, B.; Chen, W.; Wong, M. W.; Gonzalez, C.; Pople, J. A. *Gaussian 03*; Gaussian, Inc.: Wallingford, CT, 2003.
(52) Becke, A. D. *Phys. Rev. A* **1988**, *38*, 3098−3100.
(53) Perdew, J. P. *Phys. Rev. B* **1986**, *33*, 8822−8824.
(54) Perdew, J. P. *Phys. Rev. B* **1986**, *34*, 7406.
(55) Hay, P. J.; Wadt, W. R. *J. Chem. Phys.* **1985**, *82*, 270−283.
(56) Wadt, W. R.; Hay, P. J. *J. Chem. Phys.* **1985**, *82*, 284−298.
(57) Tomasi, J.; Mennucci, B.; Cammi, R. *Chem. Rev.* **2005**, *105*, 2999−3093.
(58) Otwinowski Z.; Minor W. *Macromolecular Crystallography. Part A*; Carter, C. W., Jr., Sweet, R. M., Eds.; Academic Press: San Diego, CA, 1997; Chapter 276, pp 307−326.
(59) Blessing, R. H. *Acta Crystallogr.* **1995**, *A51* (Pt 1), 33−38.
(60) Altomare, A.; Burla, M. C.; Camalli, M.; Cascarano, G. L.; Giacovazzo, C.; Guagliardi, A.; Moliterni, A. G. G.; Polidori, G.; Spagna, R. *J. Appl. Crystallogr.* **1999**, *32*, 115−119.
(61) Sheldrich G. M. SHELXTL-97, Program for the Solutiont of Crystal Structure. 1997.
(62) Nardelli, M. *J. Appl. Crystallogr.* **1995**, *28*, 659.
(63) Farrugia, L. J. *J. Appl. Crystallogr.* **1999**, *32*, 837−838.